または儀式的行動の現れの場合がある。ある子供達は自閉症に似た行動をもつ、しかし彼等は自閉症ではない。うつ病は珍しくない。とても稀に、重い精神病障害が現れる場合がある。もし親は、気分、行動、あるいは思考過程の著しい悪化に気が付いた場合、迅速に知識のある専門家による検査が行われるべきである。

ソトス症候群の子供達は、彼等の発達と社会的な挑戦のため、何らかの行動や感情障害に直面する事が珍しくない。確かに、行動困難の初期診断と結び付けられた子供達の中には、ソトス症候群と認識されていない子供達もいる。覚えておいてほしい重要な事は、これらの行動パターンは変化の対象であり、しばしば“発達年齢”と生物学上の年齢の矛盾が説明の要因にされる。もし、正式な評価が勧められたら、“レッテル”と限界が目的では無い事、しかしむしろ家庭や学校における相互作用の最も効果的な種類を計画するのを援助するものである事を忘れないようにする。行動修正プログラムは、薬を使う、使わないに関係なく、非常に役立つ可能性がある。

私はこの数年で
とてもスピリチュアルな人間になった。

私はこの世で大切なものが
－美しさ、知能、運動の才能，成功－
では無い事に気づいた。

本当に大切なのは愛、挑戦する事、
笑う事、不思議に思う事、勇気。

私の娘はそれら全てを持っている。

もし、私が娘を受け入れる事ができるなら、
そうしたら私は私自身を愛し受け入れる事ができる、
私の全ての欠点も，私の人間らしさも。

娘は私の先生。
私は常に娘の生徒。
そして私は遅のろいけれど、とてもやる気満々の学習者。

III. 研究成果の刊行に関する一覧表

研究成果の刊行に関する一覧表

書籍

著者氏名	論文タイトル名	書籍全体の編集者名	書　籍　名	出版社名	出版地	出版年	ページ
富田博秋.	遺伝子発現解析研究の実際～ブレインバンク運営に求められている品質管理とは	加藤忠史	脳バンク　精神疾患の謎を解くために	光文社	東京	2011	167-176
富田博秋.	求められるブレインバンクの姿　～ブレインバンクは実際に何をするのか～	加藤忠史	脳バンク　精神疾患の謎を解くために	光文社	東京	2011	237-245
富田博秋	精神神経疾患死後脳のバイオリソース整備. ,.	独立行政法人科学技術振興機構	研究開発戦略センター国際比較調査報告書2011年版	独立行政法人科学技術振興機構	東京	2011	126-129
富田博秋、小野千晶、兪志前	. 統合失調症の陰性症状の進行に関わる精神神経免疫学的メカニズムに関する研究	財団法人　精神・神経科学振興財団	こころの健康と病気2010年版	財団法人精神・神経科学振興財団	東京	2011	119-131
黒澤健司.	確定診断とその進め方	福嶋義光	遺伝子医学MOOK別冊「遺伝カウンセリングハンドブック」	メディカルドウ	大阪	2011	58-59
黒澤健司.	先天奇形、先天奇形症候群、Dysmorphology.	福嶋義光	遺伝子医学MOOK別冊「遺伝カウンセリングハンドブック」	メディカルドウ	大阪	2011	76-79
黒澤健司.	予想外の結果が得られた場合：次世代シークエンス	福嶋義光	遺伝子医学MOOK別冊「遺伝カウンセリングハンドブック」	メディカルドウ	大阪	2011	345-347
福與なおみ、高橋利幸、藤原一男	視神経脊髄炎	塩見正司	小児科臨床ピクシス28「急性脳炎・急性脳症」	診断と治療社	東京	2011	

雑誌

発表者氏名	論文タイトル名	発表誌名	巻号	ページ	出版年
Yoneda Y, Saitsu H, Touyama M, Makita Y, Miyamoto A, Hamada K, Kurotaki N, Tomita H, Nishiyama K, Tsurusaki Y; Doi H, Miyake N, Ogata K, Naritomi K, Matsumoto N.	Missense mutations in the DNA-binding/dimerization domain of NFIX cause Sotos-like features.	J Hum Genet.	57(3)	207-211	2012
Yu Z, Ono C, Kim HB, Komatsu H, Tanabe Y, Sakae N, Nakayama KI, Matsuoka H, Sora I, Bunney WE, Tomita H.	Four mood stabilizers commonly induce FEZ1 expression in human astrocytes	Bipolar Disorders	13(5-6)	486-499	2011
Yu Z, Ono C, Sora I, Tomita H	Effect of chronic lithium treatment on gene expression profile in mouse microglia and brain dendritic cells	Japanese Journal of Neuropsychopharmacology	31 (2)	101-102	2011
Saitsu H, Osaka H, Sasaki M, Takanashi J, Hamada K, Yamashita A,et., al., Matsumoto N.	Mutations in POLR3A and POLR3B encoding RNA polymerase III subunits cause an autosomal recessive hypomyelinating leukoencephalopathy.	Am J Hum Genet	in press		
Yoneda Y, Haginoya K, Arai H, Tsurusaki Y, et. al. , Matsumoto N, Saitsu H.	De novo and inherited mutations in the gene encoding PORE (tentative name) cause porencephaly.	Am J Hum Genet	in press		
Doi H, Yoshida K, T Yasuda, Fukuda M, Fukuda Y, et. al., Matsumoto N.	Exome sequencing reveals a homozygous SYT14 mutation in adult-onset autosomal recessive spinocerebellar ataxia with psychomotor retardation.	Am J Hum Genet	89(2)	320-327	2011
Okada I, Hamanoue H, Terada K, et. al., Matsumoto N, Saitsu H.	SMOC1 is essential for ocular and limb development in humans and mice.	Am J Hum Genet	88(1)	30-41	2011
Saitsu H, Osaka H, Sugiyama S, Kurosawa K, et., al., Kato M, Matsumoto N.	Early infantile epileptic encephalopathy associated with the disrupted gene encoding Slit-Robo Rho GTPase activating protein 2 (SRGAP2).	Am J Med Genet	in press		
Saitsu H, Kato M, Shimono M, Senju A, et. al., Matsumoto N.	Association of genomic deletions in the STXBP1 gene with Ohtahara syndrome.	Clin Genet	in press		

発表者氏名	論文タイトル名	発表誌名	巻号	ページ	出版年
Saitsu H, Igarashi N, Mitsuhiro Kato M, et. al., Hayasaka K, Matsumoto N.	De novo 5q14.3 translocation 121.5-kb upstream of MEF2C in a patient with severe mental retardation and early-onset epileptic encephalopathy.	Am J Med Genet	in press		
Kosho T, Miyake N, Mizumoto S, Hatamochi A, Fukushima Y, Sugahara K, Matsumoto N.	A response to: Loss of dermatan-4-sulfotransferase 1 (D4ST1/CHST14) function represents the first dermatan sulfate biosynthesis defect, "Dermatan sulfate-deficient adducted thumb–clubfoot syndrome". Which name is appropriate, "Adducted thumb–clubfoot syndrome" or "Ehlers–Danlos syndrome"?	Hum Mut	in press		
Saitsu H, Osaka H, Nishiyama K, Tsurusaki Y, Doi H, Miyake N, Matsumoto N.	A girl with early-onset epileptic encephalopathy associated with microdeletion involving CDKL5., in press	Brain Dev	in press		
Sakai H, Suzuki S, Mizuguchi T, Imoto K, Doi H, Kikuchi M, Tsurusaki T, Saitsu H, Miyake N, Masuda M, Matsumoto N.	Rapid detection of gene mutations responsible for non-syndromic aortic aneurysm and dissection using two different methods: resequencing microarray technology and next-generation sequencing.	Hum Genet	in press		
Abdel-Salam GMH, Miyake N, Eid MM, Abdel-Hamid MS, Hassan NA, Eid OM, Effat LK, El-Badry TH, El-Kamah GY, El-Darouti M, Matsumoto N.	A homozygous Mutation in RNU4ATAC as a cause of microcephalic osteodysplastic primordial dwarfism type I (MOPD I) with associated pigmentary disorder.	Am J Med Genet	in press		
Miyatake S, Miyake N, Touho H, et. al. Matsumoto N.	Homozygous c.14576G>A variant of RNF213 predicts early-onset and severe form of moyamoya disease.	Neurology,	in press		
Tohyama J, Kato M, N, Kawasaki S, Kawara H, Matsui T, Akasaka N, Ohashi T, Kobayashi Y, Matsumoto N.	Dandy-Walker malformation associated with heterozygous ZIC1 and ZIC4 deletion: Report of a new patient.	Am J Med Genet	155(1)	130-131	2011

発表者氏名	論文タイトル名	発表誌名	巻号	ページ	出版年
Furuichi T, Dai J, Cho T-J, et. al. Matsumoto N, et. al.	CANT1 is also responsible for Desbuquois dysplasia, type 2 and Kim variant.	J Med Genet	48(1)	32-37	2011
Saitsu H, Hoshino H, Kato M, rt, al., Matsumoto N.	Paternal mosaicism of a STXBP1 mutation in Ohtahara syndrome.	Clin Genet	80	484-488	2011
Yano S, Bagheri A, Watanabe Y, Moseley K, Nishimura A, Matsumoto N, Baskin B, Ray PN.	Familial Simpson-Golabi-Behmel syndrome: Studies of X-chromosome inactivation and clinical phenotypes in two female individuals with GPC3 mutations.	Clin Genet	80	466-471	2011
Nishimura-Tadaki A, Wada T, Bano G, et. al., Matsumoto N.	Breakpoint determination of X;autosome balanced translocations in four patients with premature ovarian failure.	J Hum Genet	56(2)	156-160	2011
Hiraki Y, Nishimura A, Hayashidani M, Terada Y, Nishimura G, Okamoto N, Nishina S, Tsurusaki Y, Doi H, Saitsu H, Miyake N, Matsumoto N.	A de novo deletion of 20q11.2-q12 in a boy presenting with abnormal hands and feet, retinal dysplasia, and intractable feeding difficulty.	Am J Med Genet	152(2)	409-414	2011
Tonoki H, Harada N, Shimokawa O, Yosozumi A, Monzaki K, Satoh K, Mika Kosaki R, Sato A, Matsumoto N, Iizuka S.	Axenfeld-Rieger anomaly and Axenfeld-Rieger syndrome: clinical, molecular-cytogenetic, and DNA array analyses on three patients with chromosomal defects at 6p25.	Am J Med Genet Part A:	155 (12)	2925-2932	2011
Tadaki H, Saitsu H, Nishimura-Tadaki A, et. al., Matsumoto N.	De novo 19q13.42 duplications involving NLRP gene cluster in a patient with systemic-onset juvenile idiopathic arthritis.	J Hum Genet	56	343-347	2011
Miyake N, Yamashita S, Kurosawa K, et. al. Matsumoto N.	A novel homozygous mutation of DARS2 may cause a severe LBSL variant.	Clin Genet	80(3)	293-296	2011
Tadaki H, Saitsu H, Kanegane H, Miyake N, et. al., Matsumoto N.	Exonic deletion of CASP10 in a patient presenting with systemic juvenile idiopathic arthritis, but not with autoimmune lymphoproliferative syndrome type IIa.	Int J Immunogenet	38	287-293	2011

発表者氏名	論文タイトル名	発表誌名	巻号	ページ	出版年
Tsurusaki Y, Osaka H, Hamanoue H, Shimbo H, Tsuji M, Doi H, Saitsu H, Matsumoto N, Miyake N.	Rapid detection of a mutation causing X-linked leukodystrophy by exome sequencing.	J Med Genet	48	606-609	2011
Narumi Y, Shiihara T, Yoshihasi H, et. al. Matsumoto N, Fukushima Y.	Hypomyelination with atrophy of the basal ganglia and cerebellum (H-ABC) in an infant with Down syndrome.	Clin Dysmorphol	20(3)	166-167	2011
Dai J, Kim O-K, Cho T-J, et.al. Matsumoto N, Ohashi H, Kamatani N, Nishimura G, Furuichi T, Takahashi A, Ikegawa S.	A founder mutation of CANT1 common in Korean and Japanese Desbuquois dysplasia.	J Hum Genet	56(5)	398-400	2011
Saitsu H, Matsumoto N.	Genetic commentary: De novo mutations in epilepsy.	Dev Med Child Neurol	9	806-807	2011
Shimizu K, Okamoto N, Miyake N, et. al. Matsumoto N, Kosho T.	Delineation of dermatan 4-O-sulfotransferase 1 deficient Ehlers-Danlos syndrome: Observation of two additional patients and comprehensive review of 20 reported patients.	Am J Med Genet	155(8)	1949-1958	2011
Tsurusaki Y, Okamoto N, Suzuki Y, Doi H, Saitsu H, Miyake N, Matsumoto N.	Exome sequencing of two patients in a family with atypical X-linked leukodystrophy.	Clin Genet	80	161-166	2011
Hannibal MC, Buckingham KJ, Ng SB, et.al. Matsumoto N, , et. al., Bamshad MJ.	Spectrum of MLL2 (ALR) mutations in 110 cases of Kabuki syndrome.:,	Am J Med Genet	155 (7)	1511-1516	2011
Nagase H, Ishikawa H, Nishikawa T, Kurosawa K, Itani Y, Yamanaka M.	Prenatl management of the fetus with lethal malformation: from a study of oligohydroamnios sequence.	Fetal and Pediatric Pathology	30	145-149	2011
Tachibana Y, Aida N, Enomoto K, Iai M, Kurosawa K.	A case of Sjögren-Larsson syndrome with minimal MR imaging findings facilitated by proton spectroscopy.	Pediatr Radiol,	Epub ahead of print		2011
Ozawa K, Ishikawa H, Maruyama Y, Nagata T, Nagase H, Itani Y, Kurosawa K, Yamanaka M.	Congenital omphalocele and polyhydramnios: A study of 52 cases.	Fetal Diagn Ther	Epub ahead of print		2011

発表者氏名	論文タイトル名	発表誌名	巻号	ページ	出版年
Soneda A, Teruya H, Furuya N, Yoshihashi H, Enomoto K, Ishikawa A, Matsui K, Kurosawa K.	Proportion of malformations and genetic disorders among cases encountered at a high-care unit in a children's hospital.	Eur J Pediatr	Epub ahead of print		2011
Kurosawa K, Tanoshima-Takei M, Yamamoto T, Ishikawa H, Masuno M, Tanaka Y, Yamanaka M.	Sirenomelia with a de novo balanced translocation 46,X,t(X;16)(p11.2;p12.3).	Cong Anom	in press		
Kurosawa K, Masuno M, Kuroki Y.	Trends in occurrence of twin births in Japan.	Am J Med Genet Part A	Epub ahead of print		2011
Saito Y, Kubota M, Kurosawa K, et. al.	Polymicrogyria and infantile spasms in a patient with 1p36 deletion syndrome.	Brain Dev	33	437-441	2011
Uematsu M, Haginoya K, Kikuchi A, et. al. Hino-Fukuyo NFujiwara I, Kure S.	Hypoperfusion in caudate nuclei in patients with brain–lung–thyroid syndrome.	J Neurol Sci	in press		
Hirose M, Haginoya K, Yokoyama H, Kikuchi A, Hino-Fukuyo N, et. al.	Progressive atrophy of the cerebrum in 2 Japanese sisters with microcephaly with simplified gyri and enlarged extraaxial space.	Neuropediatrics	42(4)	163-166	2011
Waga C, Okamoto N, Ondo Y, Fukumura-Kato R, Goto YI, Kohsaka S, Uchino S.	Novel variants of the SHANK3 gene in Japanese autistic patients with severe delayed speech development.	Psychiatr Genet	21	208-211	2011
Okamoto N, Hatsukawa Y, Shimojima K, Yamamoto T.	Submicroscopic deletion in 7q31 encompassing CADPS2 and TSPAN12 in a child with autism spectrum disorder and PHPV	Am J Med Genet A	155	1568-1573	2011
Hayashi S, Okamoto N, Chinen Y, Takanashi JI, Makita Y, Hata A, Imoto I, Inazawa J.	Novel intragenic duplications and mutations of CASK in patients with mental retardation and microcephaly with pontine and cerebellar hypoplasia (MICPCH).	Hum Genet	Epub ahead of print		2011

発表者氏名	論文タイトル名	発表誌名	巻号	ページ	出版年
Kawazu Y, Inamura N, Kayatani F, Okamoto N, Morisaki H.	Prenatal complex congenital heart disease with Loeys–Dietz syndrome	Cardiology in the Young	on line		2011
Naiki M, Mizuno S, Yamada K, Yamada Y, Kimura R, Oshiro M, Okamoto N, Makita Y, Seishima M, Wakamatsu N.	MBTPS2 mutation causes BRESEK/BRESHECK syndrome.	Am J Med Genet	on line		2011
Okamoto N, Tamura D, Nishimura G, Shimojima K, Yamamoto T	Submicroscopic deletion of 12q13 including HOXC gene cluster with skeletal anomalies and global developmental delay.	Am J Med Genet A	155	2997-3001	2011
Ono S, Yoshiura K, Kurotaki N, Kikuchi T, Niikawa N, Kinoshita A.	Mutation and copy number analysis in paroxysmal kinesigenic dyskinesia families.	Mov Disord	26(4)	761-763	2011
Kubo T, Horai S, Ozawa H, Kurotaki N.	A case of undiagnosed catecholaminergic polymorphic ventricular tachycardia presenting with ventricular fibrillation after administration of succinylcholine during anesthesia for modified electroconvulsive therapy.	Psychiatry Clin Neurosci	65(4)	397	2011
Kurotaki N, Nobata H, Nonaka S, Nishihara K, Ozawa H.	Three cases of schizophrenia showing improvement after switching to blonanserin.	Psychiatry Clin Neurosci	65(4)	396-397	2011
Kurotaki N, Tasaki S, Mishima H, Ono S, Imamura A, Kikuchi T, Nishida N, Tokunaga K, Yoshiura K, Ozawa H.	Identification of novel schizophrenia loci by homozygosity mapping using DNA microarray analysis.	PLoS one	6(5)	e20589	2011
富田博秋	統合失調症の死後脳研究の現状と展望	精神科治療学	26 (12)	1581-1587	2011
沼田有里佳、植松貢、福與なおみ、柿坂庸介、小林朋子、廣瀬三恵子、萩野谷和裕、土屋滋	咽頭筋麻痺を認めない咽頭頸部上腕型 Guillain-Barré 症候群の 1 例	脳と発達	43	482-485	2011

発表者氏名	論文タイトル名	発表誌名	巻号	ページ	出版年
福與なおみ、高橋利幸、萩野谷和裕、植松貢、土屋滋、藤原一男	小児期発症の抗アクアポリン4抗体陽性症例の臨床像	脳と発達	43	359-365	2011
渡邊尚子，黒滝直弘，菊池妙子，小澤寛樹.	Olanzapine投与が全身痙攣発作の原因と考えられた統合失調症の1例.	精神科	18(3)	359-365	2011
田山達之，黒滝直弘，渡邊尚子，金替伸治，小澤寛樹，木下裕久.	慢性関節リウマチに対し投与した抗IL-6受容体抗体が精神病症状の出現に関与したと考えられた1症例.	臨床精神医学	40(10)	1387-1390	2011
黒滝直弘，中根秀之.	ソトス症候群の分子遺伝解析とサポートシステムの開発における課題	精神科	in press		

IV. 研究成果の刊行物・別刷

Journal of Human Genetics (2012) 57, 207–211

www.nature.com/jhg

ORIGINAL ARTICLE

Missense mutations in the DNA-binding/dimerization domain of *NFIX* cause Sotos-like features

Yuriko Yoneda[1], Hirotomo Saitsu[1], Mayumi Touyama[2], Yoshio Makita[3], Akie Miyamoto[4], Keisuke Hamada[5], Naohiro Kurotaki[6], Hiroaki Tomita[7], Kiyomi Nishiyama[1], Yoshinori Tsurusaki[1], Hiroshi Doi[1], Noriko Miyake[1], Kazuhiro Ogata[5], Kenji Naritomi[8] and Naomichi Matsumoto[1]

Sotos syndrome is characterized by prenatal and postnatal overgrowth, characteristic craniofacial features and mental retardation. Haploinsufficiency of *NSD1* causes Sotos syndrome. Recently, two microdeletions encompassing *Nuclear Factor I-X (NFIX)* and a nonsense mutation in *NFIX* have been found in three individuals with Sotos-like overgrowth features, suggesting possible involvements of *NFIX* abnormalities in Sotos-like features. Interestingly, seven frameshift and two splice site mutations in *NFIX* have also been found in nine individuals with Marshall–Smith syndrome. In this study, 48 individuals who were suspected as Sotos syndrome but showing no *NSD1* abnormalities were examined for *NFIX* mutations by high-resolution melt analysis. We identified two heterozygous missense mutations in the DNA-binding/dimerization domain of the NFIX protein. Both mutations occurred at evolutionally conserved amino acids. The c.179T>C (p.Leu60Pro) mutation occurred *de novo* and the c.362G>C (p.Arg121Pro) mutation was inherited from possibly affected mother. Both mutations were absent in 250 healthy Japanese controls. Our study revealed that missense mutations in *NFIX* were able to cause Sotos-like features. Mutations in DNA-binding/dimerization domain of NFIX protein also suggest that the transcriptional regulation is abnormally fluctuated because of *NFIX* abnormalities. In individuals with Sotos-like features unrelated to *NSD1* changes, genetic testing of *NFIX* should be considered.
Journal of Human Genetics (2012) **57**, 207–211; doi:10.1038/jhg.2012.7; published online 2 February 2012

Keywords: DNA-binding/dimerization domain; missense mutation; *NFIX*; Sotos syndrome

INTRODUCTION

Sotos syndrome (MIM #117550) is an overgrowth syndrome characterized by tall stature and/or macrocephaly, distinctive facial appearance and mental retardation.[1] A *de novo* t(5;8)(q35;q24.1) translocation in a patient with Sotos syndrome revealed disruption of *NSD1* at 5q35. Subsequent identification of nonsense, frameshift and submicroscopic deletion mutations of *NSD1* in patients with Sotos syndrome clearly showed that haploinsufficiency of *NSD1* causes Sotos syndrome.[2] *NSD1* encodes nuclear receptor-binding SET domain protein 1, which functions as a histone methyltransferase that activates and represses transcription through chromatin modification.[3] The diagnosis of Sotos syndrome is established by confirming *NSD1* abnormalities,[4] and abnormalities of *NSD1* causes up to 90% of Sotos syndrome cases. However, a part of patients with suspected Sotos syndrome are known to show no abnormalities in *NSD1*,[5] suggesting involvement of another gene.

Recently it was reported that two patients with Sotos-like overgrowth features possessed microdeletions encompassing *Nuclear Factor I-X (NFIX)* at 19p13.2. In addition, a nonsense mutation in *NFIX* was identified in one patient with Sotos-like features.[6] Interestingly, frameshift and donor-splice site mutations were also identified in Marshall–Smith syndrome (MIM 602535) that is osteochondysplasia syndrome characterized by accelerated skeletal maturation, relative failure to thrive, respiratory difficulties, mental retardation and unusual facial features.[7] Therefore, *NFIX* mutations could cause either Sotos-like features or Marshall–Smith syndrome. Whereas the transcripts possessing the nonsense mutation in a patient with Sotos-like features suffered from the nonsense-mediated mRNA decay, transcripts of mutated alleles (by a donor-spice site and two frameshift mutations) in patients with Marshall–Smith syndrome escaped from the nonsense-mediated mRNA decay surveillance and could be translated, suggesting that haploinsufficiency of *NFIX* leads to

[1]Department of Human Genetics, Yokohama City University Graduate School of Medicine, Yokohama, Japan; [2]Department of Pediatrics, Okinawa Child Development Center, Okinawa, Japan; [3]Education Center, Asahikawa Medical University, Asahikawa, Japan; [4]Department of Pediatrics, Hokkaido Asahikawa Habilitation Center for Disabled Children, Asahikawa, Japan; [5]Department of Biochemistry, Yokohama City University Graduate School of Medicine, Yokohama, Japan; [6]Department of Neuropsychiatry, Nagasaki University Graduate School of Biomedical Sciences, Nagasaki, Japan; [7]Department of Biological Psychiatry, Tohoku University Graduate School of Medicine, Sendai, Japan and [8]Department of Medical Genetics, University of the Ryukyus Faculty of Medicine, Nishihara, Japan
Correspondence: Dr N Matsumoto, Department of Human Genetics, Yokohama City University Graduate School of Medicine, Fukuura 3-9, Kanazawa-ku, Yokohama 236-0004, Japan.
E-mail: naomat@yokohama-cu.ac.jp
Received 9 September 2011; revised 21 November 2011; accepted 5 January 2012; published online 2 February 2012

Sotos-like features and dominant-negative effects of the truncated NFIX proteins cause Marshall–Smith syndrome.[6]

In this study, we screened for *NFIX* mutations in 48 Japanese patients who were suspected as Sotos syndrome, but showed neither deletions nor mutations in *NSD1*. Detailed genetic and clinical data are presented.

MATERIALS AND METHODS

Subjects

A total of 48 patients suspected as Sotos syndrome were analyzed for *NFIX* mutations. *NSD1* investigation by sequencing and fluorescent *in situ* hybridization analysis was negative in these patients. In this study, the patients presenting with cardinal features of Sotos syndrome (specific craniofacial features, intellectual disability and overgrowth to same extent) but showing no *NSD1* abnormalities are referred as those with 'Sotos-like features'. Experimental protocols were approved by the Committee for Ethical issues at Yokohama City University School of Medicine. All individuals were investigated in agreement with the requirements of Japanese regulations.

Mutation analysis

Genomic DNA was isolated from peripheral blood leukocytes according to standard methods. DNA for mutation screening was amplified by illustra GenomiPhi V2 DNA Amplification Kit (GE Healthcare, Buckinghamshire, UK). Sequencing of exon 1 and high-resolution melting curve (HRM) analysis of exon 2–9 covering the *NFIX* coding region (GenBank accession number NM_002501.2) were performed. For exon 1, the 12 μl PCR mixture contained 30 ng DNA, 0.3 μM each primer, 0.4 mM each dNTP, 1× PCR buffer for KOD FX and 0.3 U KOD FX polymerase (Toyobo, Osaka, Japan). For exons 2–9, real-time PCR and HRM analysis were serially performed in 12 μl mixture on Rotor-Gene Q (QIAGEN, Hilden, Germany). For exon 7, the PCR mixture contained 30 ng DNA, 0.3 μM each primer, 0.4 mM each dNTP, 0.36 μl SYTO9 (Invitrogen, Carlsbad, CA, USA), 0.4 mM each dNTP, 1× PCR buffer for KOD FX and 0.3 U KOD FX polymerase (Toyobo). For the remaining exons, the PCR mixture contained 30 ng DNA, 0.25 μM each primer, 0.36 μl SYTO9 (Invitrogen), 0.2 mM each dNTP, 1× ExTaq buffer and 0.375 U ExTaq HS (Takara, Otsu, Japan). Primers and conditions of PCR are shown in Supplementary Table 1. The PCR products showing an aberrant melting curve were sequenced. All the novel mutations in DNA amplified by GenomiPhi were verified by sequencing of PCR products using genomic DNA as a template. Mutations were checked in 250 Japanese normal controls (500 alleles) by HRM analysis.

Parentage testing

For the family showing *de novo* mutations, parentage was confirmed by microsatellite analysis as previously described.[8] Biological parentage was judged if more than four informative markers were compatible and other uninformative markers showed no discrepancies.

Prediction of functional effect

The effect of the mutations for protein features was predicted by following web-based prediction tools: SIFT (http://sift.jcvi.org/), PolyPhen (http://genetics.bwh.harvard.edu/pph/), PolyPhen-2 (http://genetics.bwh.harvard.edu/pph2/), Mutation Taster (http://www.mutationtaster.org/) and Align GVGD (http://agvgd.iarc.fr/agvgd_input.php).

RESULTS

NFIX mutations

Two heterozygous missense mutations were identified. The c.179T>C (p.Leu60Pro) mutation in patient 1 were not found in her parents, indicating that the mutation occurred *de novo* (Figure 1a). Biological parentage was confirmed by several microsatellite markers (data not shown). The c.362G>C (p.Arg121Pro) mutation in patient 2 was found in his mother (Figure 1a). These two mutations occurred at evolutionary conserved amino acids (Figure 1b) and were absent in 250 Japanese normal controls. Interestingly, the missense changes were located in DNA-binding/dimerization domain of the NFIX protein (Figure 1c). Evaluation with web-based prediction tools strongly suggested that these substitutions are pathogenic (Supplementary Table 2).

Clinical information of the patients

Patient 1 is a product of unrelated healthy parents. The body weight at birth was 2816 g (−0.6 s.d.), height 48.8 cm (0 s.d.) and OFC 33.5 cm (+0.3 s.d.). Neonatal hypotonia was recognized. At 17 months of age, her weight was 9.24 kg (−0.5 s.d.), height 84.9 cm (+2 s.d.) and OFC 48 cm (+1.2 s.d.). The facial appearance showed long/narrow and triangular face, high forehead, midface hypoplasia, prominent ears, epicanthal folds, strabismus, down-slanting palpebral fissures, short nose with anteverted nares, prominent long philtrum, everted lower lip and narrow palate (Figure 1d). Large hands/feet, prominent fingertips, pectus excavatum were also noted. Her primary dentition started at 7 months of age and was completed by 17 months of age. Bone age was estimated as 3 years at 17 months of age and as 5 years at 3 years of age. Bullet-shaped phalanges, which are typical features of Marshall–Smith syndrome, were not observed. She was initially diagnosed as Sotos syndrome. She showed mental retardation and severe developmental delay with developmental quotients of 19. Scoliosis was noted at 18 months of age and surgically treated for several times. Complex partial seizures were noted at 4 years of age and were controlled with phenytoin and zonisamide. At present (17 years of age), prognathia was observed (Figure 1e). Her weight was 40 kg (−2 s.d.) and height 156.5 cm (−0.2 s.d.).

Patient 2 is a male at age of 20 years. The birth weight was 2938 g (−0.4 s.d.), height 51 cm (+0.8 s.d.) and OFC 35.5 cm (+1.4 s.d.). Respiratory insufficiency was noted, but no visceral malformations were pointed out. Bilateral tubing therapy was performed for recurrent bilateral exudative otitis media at 4 years of age. At 14 years of age, his weight was 58.1 kg (+0.6 s.d.) and height 185.7 cm (+3.5 s.d.). Mental retardation was evident as the IQ score (Tanaka–Binet intelligence test) was 59. Craniofacial features included high forehead, down-slanting palpebral fissures and prognathia. He was suspected as Sotos syndrome. His mother showed tall stature, suggesting that c.362G>C led to overgrowth in the mother. Unfortunately, further details of clinical features in the mother are unavailable. Clinical information of two patients is summarized in Table 1.

DISCUSSION

NFIX is a member of the nuclear factor I (NFI) family proteins, which are implicated as site-specific DNA-binding proteins known to function in viral DNA replication and gene expression regulation.[9] NFI proteins form homo- or heterodimers and bind to the palindromic DNA consensus sequence through its N-terminal DNA-binding/dimerization domain.[10] Point mutations in DNA-binding/dimerization domain of NFI protein have been shown to cause loss of dimerization, DNA-binding and replication activities,[11] highlighting the importance of structural integrity of DNA-binding/dimerization domain. It has been reported that the DNA binding domain of SMADs and NFI transcription factors shared considerable structural similarity, and the secondary structure of the DNA-binding domain of NFI was estimated based on that of SMADs.[12] In this study, we identified two heterozygous missense mutations, the c.179T>C (p.Leu60Pro) and the c.362G>C (p.Arg121Pro), in the DNA-binding/dimerization domain. Of note, two mutations are estimated to be localized within α-helical region of DNA-binding domain and at evolutionally conserved amino acids between SMADs and NFI.[12] In addition, two mutations cause substitutions to a proline residue,

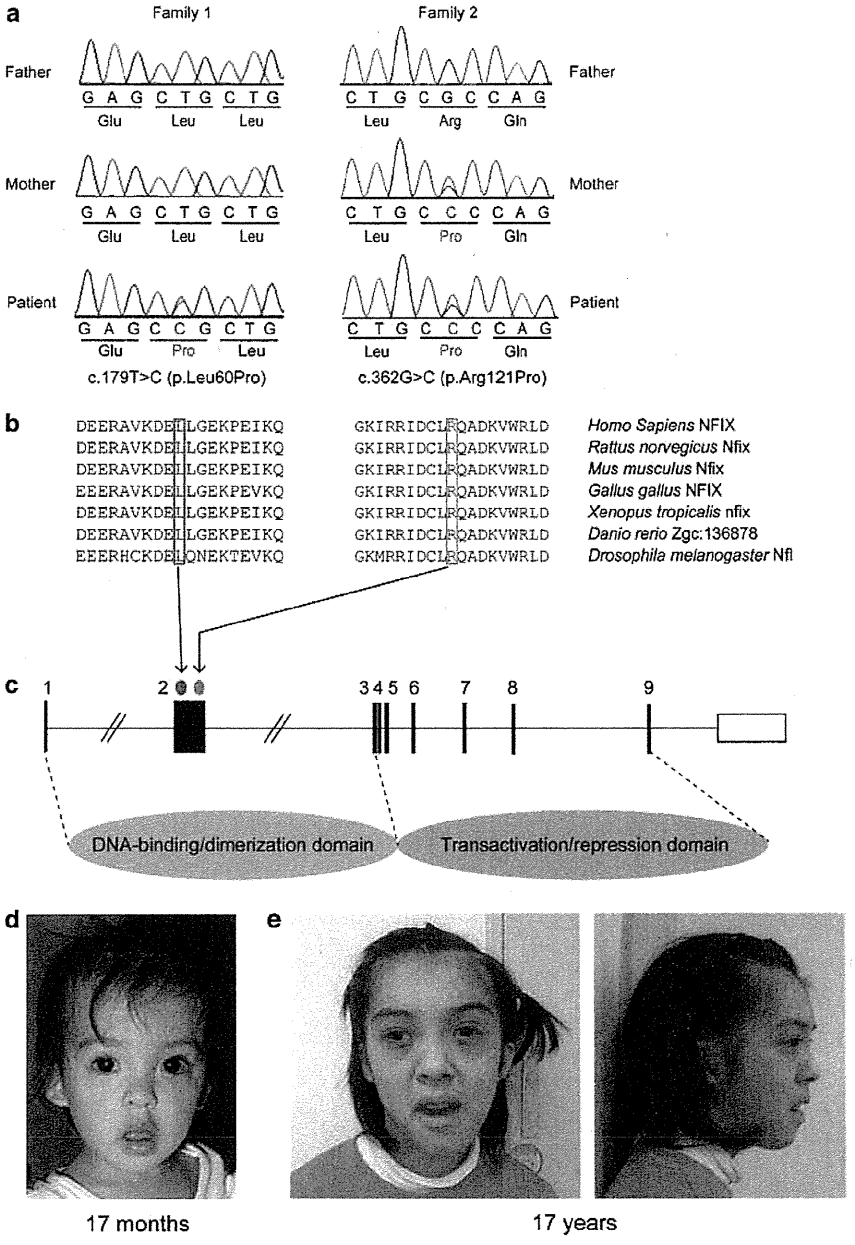

Figure 1 Missense mutations in *NFIX* in individuals with Sotos-like features. (**a**) Electropherogram of family 1 (left) and family 2 (right). The c.179T>C (p.Leu60Pro) mutation occured *de novo*. The c.362G>C (p.Arg121Pro) mutation was inherited from his mother. (**b**) An amino-acid sequence alignments of NFIX protein including amino-acid positions 60 and 121. Protein sequences were obtained through the NCBI protein database and multiple sequence alignment was performed by CLUSTALW web site (http://clustalw.ddbj.nig.ac.jp/). (**c**) Schematic representation of *NFIX* consisting of nine exons. UTR and coding exons are indicated by open and filled rectangles, respectively. The location of mutations is indicated by red (c.179T>C) and blue (c.362G>C) dots. At the bottom, C-terminal DNA-binding/dimerization domain and N-terminal transactivation/repression domain are depicted. Both the c.179T>C and c.362G>C mutations are located in exon 2 encoding a part of DNA-binding/dimerization domain. (**d**) Facial appearance of patient 1 at 17 months of age, showing long/narrow and triangular face, down slanting, short nose with anteverted nares and everted lower lip. (**e**) At 17 years of age, prognathia was noted in patient 1.

which is a unique amino acid characterized by imino radical. Proline has a pyrrolidine ring that restricts the available conformational space; therefore, it has effects on chain conformation and the process of protein folding.[13] Thus, it is very likely that two mutations could affect DNA-binding activity of NFIX protein through conformational changes of the DNA-binding domain.

Because *NFIX* mutations could cause both Marshall–Smith syndrome and Sotos-like features,[6] it is great concern to which of them two patients with missense mutations could be classified. Main clinical features of Sotos syndrome are childhood overgrowth including tall stature and/or macrocephaly, characteristic face and mental retardation. Other minor features are scoliosis, hypotonia in infancy, seizures,

Table 1 Clinical features of two patients with missense mutations in *NFIX*

				Reported by Malan et al.[6]		
		Patient 1	*Patient 2*	*Patient A*	*Patient B*	*Patient C*
Genetics	*NFIX deletion/mutation*	*c.179T>C*	*c.362G>C*	*del 19p13.3*	*del 19p13.3*	*c.568C>T*
Epidemiology	Age at last evaluation (years)	17	14	14	10	27
	Sex	F	M	M	M	F
	Mat/pat age	48/52	?/?	31/33	25/30	31/31
Prenatal growth	Birth weight (g)	2816 (−0.6 s.d.)	2938 (−0.4 s.d.)	4500 (>95)	3110 (10–50)	3600 (50–90)
	Birth height (cm)	48.8 (0 s.d.)	51 (+0.8 s.d.)	53 (95)	49 (50)	52 (95)
	OFC (cm)	33.5 (+0.3 s.d.)	35.5 (+1.4 s.d.)	38 (>95)	33.5 (10)	37.5 (>95)
Postnatal growth	Weight (kg)	9.24 (−0.5 s.d.)[a]	58.1 (+0.6 s.d.)[b]	>P98	>P98	>P98
	Height (cm)	84.9 (+2 s.d.)[a]	185.7 (+3.5 s.d.)[b]	>P98	>P98	>P98
Development						
SS	Autistic traits	−	−	+	+	+
	Behavioral anomalies	NA	−	+	+	+
	Motor retardation	+	+	+	−	−
	Hypotonia	+	+	+	+	−
Overlapped	Mental retardation	+	+	+	+	+
	Degree of delay	DQ19	IQ42	NA	NA	NA
	Speech delay	+	+	+	+	+
	First words (months)	24	18	NA	NA	NA
Craniofacial features						
SS	Long/narrow face	+	−	+	+	+
	Down-slanting palpebral fissures	+	+	+	−	+
	Small mouth	NA	−	+	−	+
	Prognathia	+	+	+	−	−
Overlapped	High forehead	+	+	+	+	+
MSS	Everted lower lip	+	−	+	−	+
	Underdeveloped midface	+	−	NA	NA	NA
	Proptosis	NA	−	NA	NA	NA
	Short nose	+	−	NA	NA	NA
	Prominent premaxilla	NA	−	NA	NA	NA
	Gum hypertrophy	+[c]	−	NA	NA	NA
	Retrognathia	−	−	NA	NA	NA
Eyes						
SS	Hypermotropia	−	−	+	+	−
	Strabismus	+	−	+	−	+
	Nystagmus	−	−	−	−	+
	Astigmatism	NA	NA	−	+	−
MSS	Myopia	NA	−	NA	NA	NA
	Blue sclerae	NA	−	NA	NA	NA
Musculo-skeletal abnormalities						
SS	Abdominal wall hypotonia	−	−	+	−	+
	Pectus excavatum	+	−	+	+	−
	Coxa valga	−	−	+	+	−
Overlapped	Scoliosis	+	−	+	−	+
	Advanced bone age	+	NA	+	+	+
MSS	Abnormal bone maturation	NA	NA	NA	NA	NA
	Bone fractures	−	−	NA	NA	NA
	Kyphosis	−	−	NA	NA	NA
	Umbilical hernia	−	−	NA	NA	NA

Abbreviations: F, female; M, male; Mat/pat, maternal/paternal; MSS, Marshall–Smith syndrome; NA, not ascertained; OFC, Occipitofrontal circumference; SS, Sotot's syndrome.
Growth of patients 1 and 2 is indicated with s.d. and that of patients in the report of Malan *et al.*[6] is indicated with percentile.
[a]At 17 months.
[b]At 14 years.
[c]Suggested the possibility of the adverse drug reaction.

cardiac defect and genitourinary anomalies.[5] On the other hand, main clinical features of Marshall–Smith syndrome are moderate to severe developmental delay with absent or limited speech, unusual behavior, disharmonic bone maturation, respiratory compromise secondary to upper airway obstruction, short stature and kyphoscoliosis.[14] One of remarkable differences between Sotos syndrome and Marshall–Smith syndrome is facial appearances. Although both syndromes has high forehead, Sotos syndrome has a long/narrow face, triangular shaped face with a prominent chin, down-slanting of the palpebral fissures,[1,4–5] whereas Marshall–Smith syndrome has proptosis, underdeveloped midface and prominent premaxilla.[7,14] In patient 1, although some characteristic features of Marshall–Smith syndrome such as everted lower lip, short nose and midface hypoplasia were observed, overall facial appearance, overgrowth features at 17 month of age, scoliosis, hypotonia and seizures were consistent with Sotos syndrome. Similarly, in patient 2, the facial appearance, tall stature and macrocephaly were consistent with Sotos syndrome. In both patients, their body weights were relatively low in comparison with their heights. This is consistent with the fact that, throughout childhood and early adolescence, the height was usually more significantly increased than weight in Sotos patients.[15] In addition, our patients did not show respiratory difficulties, one of specific features in Marshall–Smith syndrome, which cause early death in the neonatal period or early infancy.[7] Thus missense mutations in the DNA-binding/dimerization domain, which may lead to loss of transcriptional regulation by NFIX protein, could cause Sotos-like syndrome in two patients.

Many clinical features including tall statue, mental retardation, speech delay and high forehead are shared between our patients and three patients reported by Malan *et al.*[6] with *NFIX* abnormalities. The recognizable difference is autistic traits. Autistic traits are not observed in our patients but all of Malan *et al.*'s[6] patients. Thus there is a possibility that autistic traits are caused by haploinsufficiency of *NFIX* in Malan *et al.*'s[6] patients, but not by misssense mutations in the DNA-binding/dimerization domain. However, identification of a greater number of cases with *NFIX* mutations is required to confirm this hypothesis.

In conclusion, our report provides further evidences that *NFIX* is a causative gene for Sotos-like features. Abnormalities of *NSD1* are found in majority of Sotos syndrome cases and aberration of other genes including *NFIX* may be found in the minority of Sotos syndrome/Sotos-like features. Genetic testing of *NFIX* should be considered in such patients if no *NSD1* abnormalities were identified.

CONFLICT OF INTEREST

The authors declare no conflict of interest.

ACKNOWLEDGEMENTS

We thank the patients and their family members for their participation in this study. This work was supported by Research Grants from the Ministry of Health, Labour and Welfare (HS, N Miyake and N Matsumoto) and the Japan Science and Technology Agency (N Matsumoto), a Grant-in-Aid for Young Scientist from the Japan Society for the Promotion of Science (HS, HD and N Miyake) and a Grant-in-Aid for Scientific Research from Japan Society for the Promotion of Science (N Matsumoto).

1 Leventopoulos, G., Kitsiou-Tzeli, S., Kritikos, K., Psoni, S., Mavrou, A., Kanavakis, E. *et al.* A clinical study of Sotos syndrome patients with review of the literature. *Pediatr. Neurol.* **40,** 357–364 (2009).
2 Kurotaki, N., Imaizumi, K., Harada, N., Masuno, M., Kondoh, T., Nagai, T. *et al.* Haploinsufficiency of *NSD1* causes Sotos syndrome. *Nat. Genet.* **30,** 365–366 (2002).
3 Rayasam, G. V., Wendling, O., Angrand, P. O., Mark, M., Niederreither, K., Song, L. *et al. NSD1* is essential for early post-implantation development and has a catalytically active SET domain. *EMBO J.* **22,** 3153–3163 (2003).
4 Visser, R. & Matsumoto, N. in *Inborn Errors of Development* (eds Epstein, C. J., Erickson, R. P., Wynshaw-Boris, A.) 1032–1037 (Oxford University Press, New York, 2008).
5 Tatton-Brown, K. & Rahman, N. Sotos syndrome. *Eur. J. Hum. Genet.* **15,** 264–271 (2007).
6 Malan, V., Rajan, D., Thomas, S., Shaw, A. C., Louis Dit Picard, H., Layet, V. *et al.* Distinct effects of allelic *NFIX* mutations on nonsense-mediated mRNA decay engender either a Sotos-like or a Marshall-Smith syndrome. *Am. J. Hum. Genet.* **87,** 189–198 (2010).
7 Adam, M. P., Hennekam, R. C., Keppen, L. D., Bull, M. J., Clericuzio, C. L., Burke, L. W. *et al.* Marshall-Smith syndrome: natural history and evidence of an osteochondrodysplasia with connective tissue abnormalities. *Am. J. Med. Genet. A.* **137,** 117–124 (2005).
8 Saitsu, H., Kato, M., Mizuguchi, T., Hamada, K., Osaka, H., Tohyama, J. *et al. De novo* mutations in the gene encoding STXBP1 (MUNC18-1) cause early infantile epileptic encephalopathy. *Nat. Genet.* **40,** 782–788 (2008).
9 Gronostajski, R. M. Roles of the NFI/CTF gene family in transcription and development. *Gene* **249,** 31–45 (2000).
10 Kruse, U. & Sippel, A. E. Transcription factor nuclear factor I proteins form stable homo- and heterodimers. *FEBS Lett.* **348,** 46–50 (1994).
11 Armentero, M. T., Horwitz, M. & Mermod, N. Targeting of DNA polymerase to the adenovirus origin of DNA replication by interaction with nuclear factor I. *Proc. Natl. Acad. Sci. USA* **91,** 11537–11541 (1994).
12 Stefancsik, R. & Sarkar, S. Relationship between the DNA binding domains of SMAD and NFI/CTF transcription factors defines a new superfamily of genes. *DNA Seq.* **14,** 233–239 (2003).
13 MacArthur, M. W. & Thornton, J. M. Influence of proline residues on protein conformation. *J. Mol. Biol.* **218,** 397–412 (1991).
14 Shaw, A. C., van Balkom, I. D., Bauer, M., Cole, T. R., Delrue, M. A., Van Haeringen, A. *et al.* Phenotype and natural history in Marshall-Smith syndrome. *Am. J. Med. Genet. A* **152A,** 2714–2726 (2010).
15 Cole, T. R. & Hughes, H. E. Sotos syndrome: a study of the diagnostic criteria and natural history. *J. Med. Genet.* **31,** 20–32 (1994).

Supplementary Information accompanies the paper on Journal of Human Genetics website (http://www.nature.com/jhg)

BIPOLAR DISORDERS
AN INTERNATIONAL JOURNAL OF PSYCHIATRY AND NEUROSCIENCES

Bipolar Disorders 2011: 13: 486–499

Original Article

Four mood stabilizers commonly induce FEZ1 expression in human astrocytes

Yu Z, Ono C, Kim HB, Komatsu H, Tanabe Y, Sakae N, Nakayama KI, Matsuoka H, Sora I, Bunney WE, Tomita H. Four mood stabilizers commonly induce FEZ1 expression in human astrocytes. Bipolar Disord 2011: 13: 486–499. © 2011 The Authors. Journal compilation © 2011 John Wiley & Sons A/S.

Objectives: Mood stabilizers influence the morphology, chemotaxis, and survival of neurons, which are considered to be related to the mood-stabilizing effects of these drugs. Although previous studies suggest glial abnormalities in patients with bipolar disorder and an effect of mood stabilizers on certain genes in astrocytes, less is known about the effects of mood stabilizers in astrocytes than in neurons. The present study identifies a common underlying response to mood stabilizers in astrocytes.

Methods: Human astrocyte-derived cells (U-87 MG) were treated with the four most commonly used mood stabilizers (lithium, valproic acid, carbamazepine, and lamotrigine) and subjected to microarray gene expression analyses. The most prominently regulated genes were validated by qRT-PCR and western blot analysis. The intercellular localization of one of these regulated genes, fasciculation and elongation protein zeta 1 (FEZ1), was evaluated by immunofluorescence staining.

Results: The microarray data indicated that FEZ1 was the only gene commonly induced by the four mood stabilizers in human astrocyte-derived cells. An independent experiment confirmed astrocytic FEZ1 induction at both the transcript and protein levels following mood stabilizer treatments. FEZ1 localized to the cytoplasm of transformed and primary astrocytes from the human adult brain.

Conclusions: Our data suggest that FEZ1 may play important roles in human astrocytes, and that mood stabilizers might exert their cytoprotective and mood-stabilizing effects by inducing FEZ1 expression in astrocytes.

Zhiqian Yu[a], Chiaki Ono[a], Helen B Kim[b], Hiroshi Komatsu[a,c], Yoichiro Tanabe[a,c], Nobutaka Sakae[d], Keiichi I Nakayama[e], Hiroo Matsuoka[c], Ichiro Sora[a], William E Bunney[b] and Hiroaki Tomita[a]

[a]Department of Biological Psychiatry, Tohoku University Graduate School of Medicine, Sendai, Japan, [b]Department of Psychiatry and Human Behavior, University of California, Irvine, Irvine, CA, USA, [c]Department of Psychiatry, Tohoku University Graduate School of Medicine, Sendai, [d]Department of Neurology, Neurological Institute, [e]Department of Molecular and Cellular Biology, Medical Institute of Bioregulation, Kyushu University, Fukuoka, Japan

doi: 10.1111/j.1399-5618.2011.00946.x

Key words: astrocyte – bipolar disorder – carbamazepine – FEZ1 – lamotrigine – lithium – mood stabilizer – valproic acid

Received 20 August 2010, revised and accepted for publication 3 June 2011

Corresponding author:
Hiroaki Tomita, M.D., Ph.D.
Department of Biological Psychiatry
Tohoku University Graduate School of Medicine
2-1 Seiryo-machi, Aoba-ku
Sendai, 980-8575, Japan
Fax: 81-22-717-7809
E-mail: htomita@med.tohoku.ac.jp

Mood stabilizers, such as lithium (Li), valproic acid (VPA), carbamazepine (CBZ), and lamotrigine (LTG), are effective in ameliorating manic and depressive symptoms and in preventing the relapse and recurrence of bipolar disorder (BD). Mood stabilizers have significant effects on the cell survival, morphology, and chemotaxis of neuronal cells, and the neuroprotective effects of mood stabilizers are considered to be related to the mood-stabilizing effects of the drugs (1). For example, Li, VPA, and CBZ inhibit growth cone collapse and increase the spread area of growth cones (2). Various molecules, such as β-arrestin 2, glycogen synthase kinase-3 and phosphatidylinositol signaling pathways, and histone deacetylases, have been suggested as candidate targets of mood stabilizers (3–7). Evidence also suggests that the drugs exert mood-stabilizing and neuroprotective effects by altering the transcriptional regulation of various genes in the brain, including B-cell lymphoma 2 (BCL2) and ionotropic glutamate receptors type AMPA 1 (GRIA1) and type

The authors of this paper do not have any commercial associations that might pose a conflict of interest in connection with this manuscript.

AMPA 2 (GRIA2) (8, 9), potentially as downstream effectors of the target molecules of mood stabilizers.

Since these previous studies investigating the molecular mechanisms of mood stabilizers focused primarily on neuronal cells and used either neuronal cells or brain tissues, which are heterogeneous mixtures of various types of neuronal, glial, and vascular cells, the biological effects of mood stabilizers on astrocytes remain largely unknown. Since the function of astrocytes includes regulation of the extracellular concentrations of ion and neurotransmitters, modification of synaptic efficacy, maintenance of the blood-brain barrier, and structural as well as trophic support of neurons and oligodendrocytes (10–14), it is reasonable to expect that mood stabilizers may exert at least part of their mood-stabilizing and neuroprotective effects by affecting these astrocytic functions. Indeed, some studies suggest the potential involvement of astrocytes in the pathogenesis of BD. Many postmortem brain studies of patients with BD have demonstrated abnormalities in the density and shape of glial cells, as well as decreased levels of the astrocyte marker, glial fibrillary acidic protein (GFAP) (15). Glia are markedly reduced in the subgenual prefrontal cortex of patients with BD, and this reduction is most prominent in patients with familial BD (16). Mean glial density is significantly reduced in sublayers IIIc and Vb of the prefrontal cortex in patients with BD, whereas the mean size of glial cell bodies is increased in layers I and IIIc, which can be attributed to the increased density of extra-large glia in those layers (17). Although previous studies have also shown that the density and size of cortical neurons are reduced in mood disorders, these neuronal reductions are more subtle compared to the glial alterations (18). Furthermore, astrocyte-specific GFAP transcripts are significantly decreased in white matter, and tend to be decreased in gray matter of the anterior cingulate cortex of patients with BD (19). The decrease in GFAP expression was confirmed in a proteomic study of the frontal cortex of patients with BD (20). S100B, which is produced and secreted by astrocytes, is significantly increased in the serum of patients during episodes of manic and depressive states (21). S100B exerts trophic and/or toxic effects on neuronal and glial cells depending on its concentration and has been reported to be a susceptibility gene for a subgroup of BD patients presenting with psychotic symptoms (22). Thus, while current evidence is not conclusive, it does seem to suggest that a dysfunction or a loss of astrocytes may at least in part underlie the pathogenesis of BD.

Moreover, several studies have shown that mood stabilizers exert biological effects on astrocytes. Li has been shown to suppress the extracellular signal-regulated protein kinase pathway (23), whereas VPA increases the expression of neurotrophic factors in astrocytes (24). Li, VPA, and CBZ decrease *myo*-inositol uptake activity (25) and kainate receptor subunit GluR6 (GRIK2) expression in astrocytes (26), whereas Li, VPA, and CBZ increase the pH and cytosolic phospholipase A2 (cPLA2) levels in astrocytes (27, 28). It is worth noting that while these mood stabilizers have distinct chemical characteristics, they affect common molecular and cellular pathways in astrocytes.

Taken together, these studies suggest glial abnormalities in patients with BD and an effect of mood stabilizers on certain genes in astrocytes. However, the effects of mood stabilizers on astrocytes have been much less characterized compared to their effects on neuronal cells. To identify the most prominent biological effect of mood stabilizers on human astrocytes, we conducted microarray-based comprehensive gene expression analyses of a human astrocyte cell line treated with four major mood stabilizers, Li, VPA, CBZ, and LTG, and corresponding controls. We found a transcriptional regulation that was unique to each mood stabilizer and common molecules that were regulated by all four mood stabilizers. Fasciculation and elongation protein zeta 1 (FEZ1) was the only gene that was upregulated by all four mood stabilizers at both the mRNA and the protein expression levels. This finding points to FEZ1 as a candidate gene involved in the mechanism responsible for the mood-stabilizing effect of the tested drugs.

Materials and methods

Cell lines and cultures

The astrocyte-derived human cell line U-87 MG and the neuron-derived human cell line SK-N-SH were purchased from the American Type Culture Collection. The human oligodendroglioma cell line (OL) was a gift from Dr. Juan Carlos De La Torre from the Scripps Research Institute, La Jolla, CA, USA. Primary astrocytes from the human brain cortex (ACBRI 371) were purchased from Applied Cell Biology Research Institute, Kirkland, WA, USA. For the microarray studies, U-87 MG cells (6×10^8 cells) were suspended in 30 ml of Modified Eagle's Medium [(MEM) Sigma-Aldrich, St. Louis, MO, USA] containing 10% inactive fetal bovine serum (Biological Industries, Beit-Haemek, Israel) and divided into six plastic T75 cell culture flasks (Nalge Nunc Int., Rochester, NY, USA). Li (Kanto

Chemical, Tokyo, Japan) and VPA (Sigma-Aldrich) were dissolved directly in MEM at therapeutic concentrations of 0.75 mM and 0.5 mM, respectively. Cells cultured in non-treated (drug-free) MEM were used as controls to evaluate the effects of Li and VPA. The water-insoluble agents CBZ (Sigma-Aldrich) and LTG (Sigma-Aldrich) were dissolved in 100% dimethyl sulfoxide (DMSO) at 33.3 mM and 3.33 mM, respectively (666.6 times the final concentrations) and then resuspended into MEM at 50 μM and 5 μM, respectively, each of which is within the therapeutic range. Since the final DMSO concentration of CBZ- and LTG-containing MEM was 0.15%, control cells were cultured in MEM containing 0.15% DMSO. U-87 MG cells were evenly split into six flasks in MEM and maintained at 37°C in a humidified atmosphere containing 5% CO_2 for 18 hours. The media were replaced with MEM which included Li-, VPA-, CBZ-, LTG-, DMSO-containing, or non-treated MEM and cultured in the same chamber for five days. After a week of exposure to each condition, the media were removed from each flask, and the cells were washed and collected in phosphate buffered saline. To distinguish the biological effects of the mood stabilizers from artifacts, all of the experimental procedures were replicated following completion of the first set of experiments, and two sets of six types of cultured cells were subjected to the following microarray experiments. To validate the microarray expression data by quantitative real-time PCR (qRT-PCR), U-87 MG cells (1×10^8 cells) were cultured in the six different media in the presence or absence of mood stabilizers for five days, in the same manner as in the microarray experiment. For each conditioned medium, the cell culture was replicated in six independent T75 flasks (in total, 6 types of media × 6 replicates = 36 samples). To evaluate the effect of high-dose mood stabilizer treatments on protein levels by western blot, cells were cultured for five days with higher concentrations (near the maximum limit of the therapeutic ranges) of Li, VPA, CBZ, or LTG (1.2 mM, 1 mM, 100 μM, and 50 μM, respectively). Given the limited quantity of ACBRI371 cells, U-87 MG cells were used for microarray and qRT-PCR analyses, while ACBRI371 cells were used only to determine FEZ1 localization by immunocytochemistry.

RNA extraction and microarray experiments

Total RNA was extracted, DNase-digested, and purified using the RNeasy Mini Kit, RNase-free DNase I, and the RNeasy MinElute Cleanup Kit (Qiagen, Valencia, CA, USA). The RNA integrity number (RIN) for each RNA sample was confirmed to be > 9.8 using the Agilent 2100 Bioanalyzer (Agilent, Santa Clara, CA, USA), and the ribosomal RNA S28/S18 ratio was > 1.9. From the 12 total RNA samples, biotinylated cRNA were synthesized and applied to Illumina BeadChips according to the manufacturer's directions. In brief, biotinylated cRNA was prepared from 500 ng of total RNA using the Illumina Ambion RNA Amplification Kit (Ambion, Austin, TX, USA). The biotinylated cRNA samples were hybridized to Illumina Human-6v2 Expression BeadChips (Illumina, San Diego, CA, USA). Each BeadChip was washed and scanned with Illumina Bead Station 500X.

Data analysis and selection criteria for mood-stabilizer-regulated genes

The inter-array variation among 12 BeadChip microarrays (for 6 types of media × experimental duplication) was normalized using average normalization after subtracting the background signal intensities. The probability of observing a certain signal intensity level for a set of beads lacking specific probe-target hybridization was calculated as the detection p-value for each probe. The above procedure was performed using Illumina BeadStudio 3.1 software (Illumina). Among the 48,701 transcripts designed on the BeadChip, 11,214 transcripts with signal intensities > 20 and with detection p-values of < 0.05 in all of the 12 U-87 MG samples were considered reliably detectable, and the signal intensities of these transcripts in Li- and VPA-treated cells and in non-treated cells were compared. The signal intensities in CBZ- and LTG-treated cells and in DMSO-treated cells were also compared. Transcripts with consistent fold changes of > 1.2 or < 0.833 in both experimental duplicates were defined as *mood-stabilizer-induced* or *mood-stabilizer-suppressed* genes, respectively. Changes in mRNA expression are consistent among duplicated microarrays when altered genes are selected with a cut-off fold change of > 1.2 or < 0.833, criteria widely used in microarray analyses (29–31). The probability of observed number of overlapping genes in proportion to the expected number was calculated based on hypergeometric distribution, and a p-value of < 0.05 was considered statistically significant. Assuming that among the 48,701 probes, the number of genes altered by drugs A and B are 'a' and 'b' respectively, and effects of treatments are irrelevant, the expected number of overlapping genes between the lists of genes altered by drugs A and B is $(a \times b)/48{,}701$.

Hierarchical clustering

To evaluate similarities between the effects of mood stabilizers on expression profiles, the fold change values for the signal intensities of mood-stabilizer-treated samples, relative to the signal intensities determined for the control samples (Li/non-treated control, VPA/non-treated control, CBZ/DMSO-treated control, LTG/DMSO-treated control), were log2 transformed and subjected to an average linkage hierarchical clustering analysis using Genesis software 1.7.5 (available at http://www.genome.tugraz.at). To minimize the confounding effect of DMSO added to CBZ, LTG, and the corresponding control samples, 1,306 genes differentially expressed between the non-treated and DMSO-treated control samples with a fold change of > 1.2 or < 0.833 in at least one of the duplicated experiments were eliminated from the analyses. Among the 11,214 reliably detectable transcripts (with signal intensities > 20 and with detection p-values < 0.05 in all 12 U-87 MG samples), 9,908 transcripts, levels of which were similar between DMSO-treated and untreated samples, were subjected to hierarchical clustering analysis.

Quantitative real-time PCR experiments

Total RNA was extracted from the 36 cell samples [6 types of media (Li, VPA, CBZ, LTG, DMSO-treated control, non-treated control) × 6 replicates] in the same manner employed for the microarray experiment and subjected to cDNA synthesis with random primers using the SuperScript VILO cDNA synthesis kit (Invitrogen, Carlsbad, CA, USA). The relative copy number of each transcript in each cDNA sample was measured using specific primers and iQ SYBR Green Supermix (Bio-Rad, Hercules, CA, USA) with a CFX96 real-time PCR detection system (Bio-Rad). The PCR cycling parameters were as follows: 3 min at 95°C, followed by 40 cycles of 10 sec at 95°C and 30 sec at the annealing temperatures of 55°C to 65°C suitable for each primer set. The target genes were selected based on the microarray data and β-actin (ACTB) was used as an internal control for normalization. The forward and reverse primers for FEZ1 were 5′-GGGACTGCATGAGAC CATGT-3′ and 5′-TTGAGGGCTGTAGCCAG ACT-3′, respectively. The forward and reverse primers for RNA binding motif protein 14 (RBM14) were 5′-GCAAAGAAGTGAAGGG CAAG-3′ and 5′-AAAGCCTGCTGGTAGTC GAA-3′, respectively. The forward and reverse primers for ACTB were 5′-CACACTGTGCC CATCTACGA-3′ and 5′-CCATCTCTTGCTC GAAGTCC-3′, respectively. Threshold cycles were measured for triplicate samples. A standard curve was constructed for each assay to adjust for differences in the amplification efficiency between primer sets. Differences in the abundance of target genes relative to ACTB among Li-treated samples ($n = 6$), VPA-treated samples ($n = 6$) and their non-treated controls ($n = 6$) were evaluated by one-way analysis of variance (ANOVA) followed by the Dunnett post-hoc test. Likewise, differences in target gene expression levels among CBZ-treated samples ($n = 6$), LTG-treated samples ($n = 6$), and their DMSO-treated controls ($n = 6$) were evaluated by ANOVA.

Western blotting

U-87 MG cells treated with mood stabilizers and control samples were homogenized in phosphate buffered saline (PBS) containing Triton X-100, 4-(2-hydroxyethyl)-1-piperazineethanesulfonic acid (HEPES), bovine serum albumin, gentamicin sulfate, and a proteinase inhibitor cocktail containing 4-(2-aminoethyl) benzenesulfonyl fluoride, aprotinin, leupeptin, bestatin, and pepstatin A (all from Sigma-Aldrich). The supernatant obtained after centrifugation (10,000 × g for 10 min at 4°C) was subjected to sodium dodecyl sulfate polyacrylamide gel electrophoresis (SDS-PAGE) and western blotting with the following primary antibodies: polyclonal goat anti-FEZ1 antibody (1:10000; Abcam, Cambridge, UK) and monoclonal mouse anti-ACTB antibody (1:10000; Sigma-Aldrich). The secondary antibodies employed were horseradish peroxidase-conjugated anti-goat IgG (1:2000; Dako, Glostrup, Denmark) and anti-mouse IgG (1:5000; Jackson ImmunoResearch, West Grove, PA, USA), respectively. Chemiluminescence was detected using an Amersham ECL Plus western blotting detection kit (GE Healthcare, Waukesha, WI, USA) and a LAS-1000 luminescence image analyzer (Fujifilm, Tokyo, Japan), and the results were quantified using ImageJ 1.42 software (http://rsb.info.nih.gov/ij/).

Immunostaining

FEZ1 protein has been shown to be preferentially expressed in neurons but not in astrocytes or oligodendrocytes in the rat brain (32). However, the expression of FEZ1 protein in human brain-derived cells has not been investigated. To determine the expression of FEZ1 proteins in human brain astrocyte cells (U-87 MG and ACBRI 371), neurons (SK-N-SH) and oligodendrocytes (OL)